

## Isothermal section of Mg–Nd–Gd ternary system at 723 K

Long XIAO<sup>1</sup>, Yan ZHONG<sup>1</sup>, Cui-ping CHEN<sup>1</sup>, Ming-ming WULIU<sup>1</sup>, Tian-kuang LUO<sup>1</sup>, Li-bin LIU<sup>1,2</sup>, Kui LIN<sup>3</sup>

1. School of Materials Science and Engineering, Central South University, Changsha 410083, China;

2. Education Ministry Key Laboratory of Non-ferrous Materials Science and Engineering, Changsha 410083, China;

3. Guangxi Research Center of Analysis & Test, Nanning 530022, China

Received 20 March 2013; accepted 5 November 2013

**Abstract:** An isothermal section of the Mg–Nd–Gd ternary system at 723 K was established by diffusion triple technique and electron probe microanalysis (EPMA).  $\text{Mg}_3\text{Gd}$  and  $\text{Mg}_3\text{Nd}$  form a continuous solid solution  $(\text{Gd},\text{Nd})_3\text{Mg}$ , and a continuous solid solution  $(\text{Gd},\text{Nd})\text{Mg}$  is also formed between  $\text{MgGd}$  and  $\text{MgNd}$ .  $\text{Mg}_7\text{Gd}$ ,  $\text{Mg}_5\text{Gd}$ ,  $\text{Mg}_2\text{Gd}$ ,  $\text{Mg}_{41}\text{Nd}_5$ ,  $(\text{Gd},\text{Nd})_3\text{Mg}$  and  $(\text{Gd},\text{Nd})\text{Mg}$  are found in the ternary system. In these intermetallic phases,  $\text{Mg}_7\text{Gd}$  has been reported to be a metastable phase in previous literatures. The solubilities of Mg, Gd and Nd in all the phases were detected. Furthermore, four three-phase equilibria,  $\alpha(\text{Mg})+\text{Mg}_7\text{Gd}+\text{Mg}_{41}\text{Nd}_5$ ,  $\text{Mg}_7\text{Gd}+\text{Mg}_5\text{Gd}+\text{Mg}_{41}\text{Nd}_5$ ,  $\text{Mg}_5\text{Gd}+\text{Mg}_{41}\text{Nd}_5+(\text{Gd},\text{Nd})_3\text{Mg}$  and  $(\text{Gd},\text{Nd})_3\text{Mg}+(\text{Gd},\text{Nd})\text{Mg}+\text{Mg}_2\text{Gd}$ , were identified in the isothermal section.

**Key words:** magnesium alloy; Mg–Nd–Gd; diffusion triple; phase diagram; isothermal section

### 1 Introduction

With the development of automotive industry, lightweight construction materials are in increasing demand. As a result, magnesium alloys have received lots of attentions attributed to their high specific strength, good casting ability and recycle-ability. But the poor plasticity at room temperature and the poor creep resistance at elevated temperature limit their application. Recent research indicated that rare earth elements can improve casting properties, refine grain and enhance the high-temperature strength [1–6]. In order to better understand the effects of rare earth elements, diffusion triple technique is applied to the related systems.

In the Mg–Nd–Gd ternary system, the constituent binary phase diagrams of Mg–Nd, Mg–Gd and Gd–Nd have been fully investigated. The complete study on Mg–Nd system was accomplished by NAYEB-HASHEMI and CLARK [7]. There are four stable intermediate phases:  $\text{Mg}_{41}\text{Nd}_5$ ,  $\text{Mg}_3\text{Nd}$ ,  $\text{Mg}_2\text{Nd}$  and  $\text{MgNd}$ .  $\text{Mg}_2\text{Nd}$  can only exist above 941 K. All the other phases can exist at room temperature. The metastable

$\text{Mg}_{12}\text{Gd}$  phase was recognized by DELFINO et al [8]. It was reported that  $\text{Mg}_{12}\text{Nd}$  can only exist in the quenched alloys. Recently, the Mg–Nd binary phase diagram has been optimized by CALPHAD (calculation of phase diagram) methods [9–11]. Almost all of the data from experiments are in consistence with the calculated Mg–Nd phase diagram. The firstly reported Mg–Gd phase diagram contains four binary compounds,  $\text{Mg}_5\text{Gd}$ ,  $\text{Mg}_3\text{Gd}$ ,  $\text{Mg}_2\text{Gd}$  and  $\text{MgGd}$ . The  $\text{Mg}_5\text{Gd}$  is not a stoichiometry phase corresponding to the type of the crystal structure reported by ROKHLIN [12].  $\text{Mg}_{45}\text{Gd}_{11}$ ,  $\text{Mg}_6\text{Gd}$  and  $\text{Mg}_5\text{Gd}$  were used to express the chemical composition of  $\text{Mg}_5\text{Gd}$  phase. Recently,  $\text{Mg}_7\text{Gd}$  with an orthorhombic unit cell of  $a=0.64$  nm,  $b=2.28$  nm and  $c=0.52$  nm has been reported by NISHIJIMA et al [13]. All the binary phases and their crystal structures are summarized in Table 1.

As for the Mg–Nd–Gd, little experimental work has been done. Only the Nd can substitute for Gd in the  $\text{Mg}_5\text{Gd}$  phase, which was reported in Ref. [14]. The phase can be expressed as  $\text{Mg}_5(\text{Gd},\text{Nd})$ . In this work, the isothermal section of the Mg–Nd–Gd at 723 K is investigated by the diffusion triple technique. An complete isothermal section of this system is reported.

**Table 1** Intermediate compound phases and their crystal structures in Mg–Nd–Gd system

| Phase                            | Lattice parameter                          | Prototype                         | Pearson symbol |
|----------------------------------|--|-----------------------------------|----------------|
| Mg <sub>41</sub> Nd <sub>5</sub> | $a=b=1.4741\text{ nm}, c=1.0396\text{ nm}$ | Mg <sub>41</sub> Ce <sub>5</sub>  | <i>tI92</i>    |
| Mg <sub>3</sub> Nd               | $a=b=c=0.7397\text{ nm}$                   | BiF <sub>3</sub>                  | <i>cF16</i>    |
| Mg <sub>2</sub> Nd               | $a=b=c=0.8671\text{ nm}$                   | MgCu <sub>2</sub>                 | <i>cF24</i>    |
| MgNd                             | $a=b=c=0.3867\text{ nm}$                   | CsCl                              | <i>cP2</i>     |
| Mg <sub>12</sub> Nd              | $a=b=1.013\text{ nm}, c=0.593\text{ nm}$   | Mn <sub>12</sub> Th               | <i>Ti26</i>    |
| Mg <sub>5</sub> Gd               | $a=2.2344\text{ nm}$                       | Cd <sub>45</sub> Sm <sub>11</sub> | <i>cF*</i>     |
| Mg <sub>3</sub> Gd               | $a=0.7321\text{ nm}$                       | BiF <sub>3</sub>                  | <i>cF16</i>    |
| Mg <sub>2</sub> Gd               | $a=0.8575\text{ nm}$                       | MgCu <sub>2</sub>                 | <i>cF24</i>    |
| MgGd                             | $a=0.3812\text{ nm}$                       | CsCl                              | <i>cP2</i>     |

## 2 Experimental

The Mg–Nd–Gd diffusion triple specimens were fabricated from blocks of pure metals: 99.99% magnesium, 99.9% neodymium and 99.9% gadolinium. Firstly, the pure neodymium and gadolinium were cut into cubes and polished into fixed dimension; the prepared cubes were put in pure industrial alcohol for preservation. Meanwhile, the magnesium endothea was processed into a cubic hollow cone; the inwall of the cone was polished and preserved in pure industrial alcohol. Besides, especially designed extrusion mould and two cubic seal lid were made (Fig. 1). Then, the cubic neodymium, and gadolinium were put into the cubic hollow of the magnesium cone. The seal lids were placed on the top and the bottom of the hollow. The assembled sample (Fig. 2) was pressed at room temperature; the pressed depth was 15 mm. The diffusion triple sample was encapsulated in evacuated quartz tube back-filled with high purity argon. The sample was annealed at 723 K for 384 h. Then, the sample was taken out from heat treatment furnace quickly, and quenched in

water.

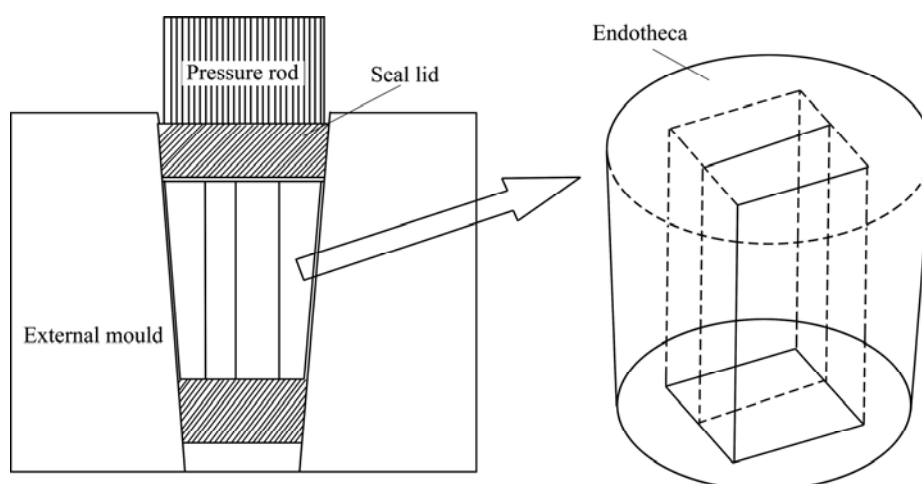
Accurate phase compositions were detected by quantitative electron probe microanalysis (EPMA) on a JEOL JXA–8800R (Japan Optics Ltd., Tokyo, Japan) microprobe with 20 kV, 20 nA, and 40° take-off angle. The electronic beam diameter was about 1  $\mu\text{m}$ .

## 3 Results and discussion

The back scattered electron (BSE) image of the Mg–Nd–Gd diffusion triple annealed at 723 K for 384 h is shown in Fig. 3. The diffusion among Mg, Nd and Gd blocks has occurred sufficiently during the long time diffusion treatment. All the equilibrium binary phases can be identified in the diffusion triple.

On the Mg–Gd side, there are seven diffusion layers in the BSE images (Fig. 3). Those layers have been identified by EPMA to be Mg, Mg<sub>7</sub>Gd, Mg<sub>5</sub>Gd, Mg<sub>3</sub>Gd, Mg<sub>2</sub>Gd, MgGd and  $\alpha$ (Gd). Mg<sub>2</sub>Gd and MgGd cannot be clearly distinguished in Fig. 3(a), but in Fig. 3(b). The thicknesses of Mg<sub>2</sub>Gd and MgGd diffusion layers are about 3  $\mu\text{m}$  and 1  $\mu\text{m}$ , respectively. According to the local equilibrium principle and the latest Mg–Gd phase diagram reported by Baikov Institute [12], there are only four binary intermediate phases, Mg<sub>5</sub>Gd, Mg<sub>3</sub>Gd, Mg<sub>2</sub>Gd and MgGd, in the binary system. So, on the Mg–Gd diffusion side, only four intermediate diffusion layers are found. But, on the Mg–Nd side of the diffusion triple five intermediate diffusion layers are found. Besides the four equilibrium phases, the stoichiometric ratio of the other phase is regarded as Mg<sub>7</sub>Gd. The minimum and maximum contents of Gd in the Mg<sub>7</sub>Gd phase are 11.5% and 12.8% in molar fraction, respectively.

According to the reports of NISHIJIMA et al [13] and LIU et al [15],  $\beta'$ -Mg<sub>7</sub>Gd is regarded as a metastable phase in the Mg–Gd alloys. But in some Mg–Nd–Gd alloys, precipitation sequences observed during aging were: Mg $\rightarrow\beta''\rightarrow\beta'$  [16], and the obtained formation

**Fig. 1** Illustration of specially designed extrusion mould for Mg–Nd–Gd diffusion triple

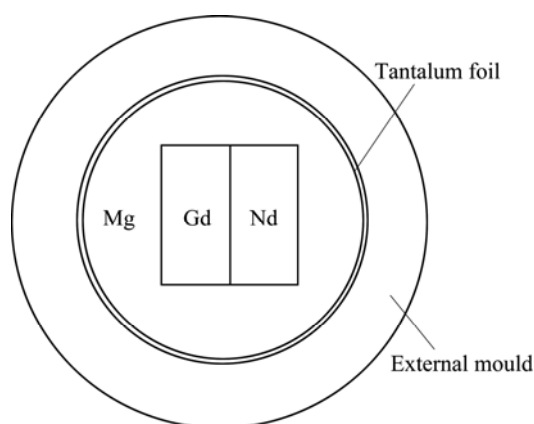


Fig. 2 Sketch of assembled sample

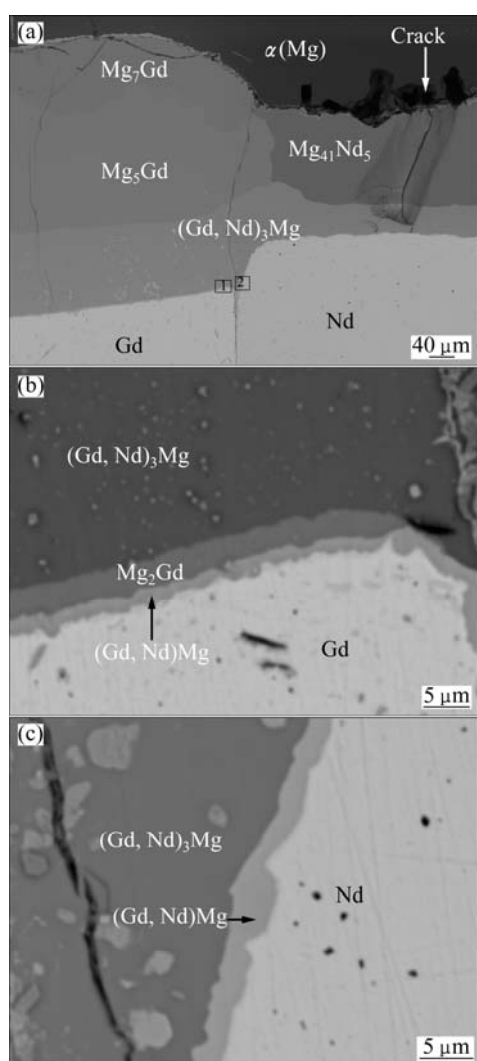


Fig. 3 BSE images of Mg–Nd–Gd system annealed at 723 K: (a) Panorama view; (b) High-magnification image of area 1; (c) High-magnification image of area 2

energy via the first-principles calculation indicated that the  $Mg_7Gd$  is energetically favorable [17]. So, the existence of the  $Mg_7Gd$  layer in the diffusion triple can be explained that the  $\beta'$ - $Mg_7Gd$  is stable compared with

almost all of the metastable phases. The  $Mg_7Gd$  phase in the diffusion triple can exist for 16 d or more at 723 K.

The last experiment data of the solubility of Gd in  $\alpha(Mg)$  reported by ROKHLIN [12] are 3.5% at 773 K and 1.8% at 673 K. The present result is 3.5% at 723 K. The solubility of Gd in  $\alpha(Mg)$  agrees well with the literature data. The  $Mg_5Gd$ ,  $Mg_3Gd$  and  $MgGd$  have definite composition range. The solubility ranges of Gd in  $Mg_5Gd$  and  $Mg_3Gd$  phase are 11.4%–17.8%, and 24.6%–25.7%, respectively. The solubility value of Gd in  $MgGd$  is ~49.2%.

Similarly, three layers of compounds have been detected on the Mg–Nd side,  $Mg_{41}Nd_5$ ,  $Mg_3Nd$  and  $MgNd$ , as shown in Figs. 3(a) and (c). The solubility of Nd in solid  $\alpha(Mg)$  was researched by ROKHLIN [12] with microscopy observation and electrical resistivity measurements previously. The solubility is 0.38% Nd at 773 K, 0.12% Nd at 673 K. The solubility of Nd in solid Mg detected in the present triple at 723 K is 0.3%. This result is in consistence with the result in Ref. [12].

$Mg_2Nd$  is not found because it has decomposed below 941 K and the  $Mg_{12}Nd$  metastable phase, which only presents as precipitates in quenched sample, is not detected also. This result is identical with the reports by MENG et al [10] and GUO and DU [11]. Both  $Mg_{41}Nd_5$  and  $Mg_3Nd$  have a little composition range. The solubility of Nd in  $Mg_{41}Nd_5$  is between 9.2% and 10.7%. The solubility of Nd in  $Mg_3Nd$  is ~24.6%.

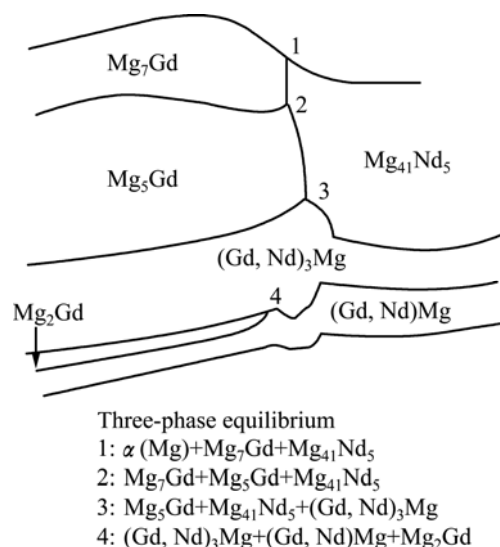
A big crack is found on the Mg–Gd side of the diffusion triple because the brittle intermediate compounds layers are broken down when the sample are polished. Fortunately, those defects do not affect the continuity of phase regions. The diffusion triple is integrated in most important areas. Owing to different phases having different diffusion rates, the thicknesses of the diffusion layers are different. There are three obvious three-phase reaction points in the BSE image in Fig. 3(a), the other in the amplified region 1 of Fig. 3(a) is shown in Fig. 3(b).

The EPMA measurements were applied at a short distance along lines perpendicular to the phase interfaces. Many groups of composition profiles can be acquired. Subsequently, a series of the two-phase equilibria are confirmed by the analysis of the composition to the corresponding interface. The extrapolated local equilibrium compositions at the two-phase interface at 723 K are shown in Table 2. The number of the three-phase equilibria is four. Owing to the small phase zones near the tri-junction points and the electron scattering effect, it is very difficult to determine the three-phase equilibrium by EPMA method. So the three-phase equilibrium was only estimated according to the two-phase equilibrium. Furthermore, no ternary

**Table 2** Extrapolated local equilibrium compositions at two-phase interface at 723 K

| Phase interface                                       | $x(\text{Mg})/\%$ | $x(\text{Gd})/\%$ | $x(\text{Mg})/\%$ | $x(\text{Gd})/\%$ |
|---|-------------------|-------------------|-------------------|-------------------|
| $\alpha(\text{Mg})/\text{Mg}_7\text{Gd}$              | 97.3              | 2.5               | 89.4              | 9.3               |
|   | 97.1              | 2.4               | 89.7              | 8.8               |
|   | 97.4              | 2.1               | 89.7              | 8.8               |
|   | 97.4              | 2.2               | 89.6              | 9.1               |
| $\alpha(\text{Mg})/\text{Mg}_{41}\text{Nd}_5$         | 99.7              | 0                 | 89.9              | 0.1               |
|   | 99.7              | 0.1               | 89.4              | 0.3               |
|   | 99.6              | 0.2               | 89.5              | 0.3               |
|   | 99.7              | 0.2               | 89.6              | 0.4               |
|   | 99.5              | 0.3               | 89.5              | 0.6               |
|   | 99.5              | 0.4               | 89.5              | 0.6               |
| $\text{Mg}_7\text{Gd}/\text{Mg}_{41}\text{Nd}_5$      | 89.5              | 9.1               | 89.6              | 0.6               |
|   | 89.7              | 9.6               | 89.5              | 0.7               |
|   | 89.7              | 9.5               | 89.3              | 0.9               |
|   | 89.4              | 9.2               | 89.3              | 0.7               |
|   | 89.5              | 9.3               | 89.1              | 0.8               |
|   | 89.6              | 9.3               | 89.2              | 0.9               |
| $\text{Mg}_7\text{Gd}/\text{Mg}_5\text{Gd}$           | 86.1              | 13.8              | 83.7              | 16.2              |
|   | 86.4              | 13.3              | 83.7              | 15.9              |
|   | 86.3              | 13.0              | 83.6              | 14.2              |
|   | 86.4              | 12.9              | 83.4              | 13.7              |
|   | 86.2              | 12.7              | 83.6              | 12.6              |
|   | 86.3              | 12.7              | 83.6              | 11.8              |
| $\text{Mg}_5\text{Gd}/\text{Mg}_{41}\text{Nd}_5$      | 83.8              | 11.4              | 89.3              | 1.5               |
|   | 83.7              | 11.3              | 88.7              | 1.6               |
|   | 83.5              | 11.4              | 88.4              | 1.3               |
|   | 83.5              | 11.2              | 88.5              | 1.2               |
|   | 83.4              | 11.0              | 88.5              | 1.1               |
| $\text{Mg}_5\text{Gd}/(\text{Gd,Nd})_3\text{Mg}$      | 82.2              | 17.8              | 74.2              | 25.7              |
|   | 82.3              | 16.4              | 74.6              | 21.5              |
|   | 82.3              | 15.2              | 74.9              | 18.3              |
|   | 82.3              | 14.3              | 75.4              | 15.9              |
|   | 82.4              | 12.9              | 75.8              | 12.7              |
|   | 82.4              | 11.6              | 76.0              | 6.4               |
| $\text{Mg}_{41}\text{Nd}_5/(\text{Gd,Nd})_3\text{Mg}$ | 88.3              | 1.3               | 75.9              | 6.2               |
|   | 88.3              | 1.0               | 75.7              | 3.5               |
|   | Mg                | Gd                | Mg                | Gd                |
|   | 88.3              | 0.8               | 75.4              | 2.1               |
|   | 88.2              | 0.4               | 75.1              | 0.8               |
| $(\text{Gd,Nd})_3\text{Mg}/\text{Mg}_2\text{Gd}$      | 73.5              | 15.4              | 67.1              | 32.4              |
|   | 73.7              | 20.8              | 67.1              | 32.2              |
|   | 73.8              | 25.7              | 67.6              | 31.9              |
| $(\text{Gd,Nd})_3\text{Mg}/(\text{Gd,Nd})\text{Mg}$   | 73.4              | 14.9              | 50.6              | 49.2              |
|   | 73.2              | 11.7              | 50.3              | 40.8              |
|   | 73.5              | 8.4               | 50.7              | 28.3              |
|   | 73.9              | 5.1               | 50.5              | 11.6              |
|   | 73.5              | 1.4               | 51.1              | 0.4               |
| $\text{Mg}_2\text{Gd}/(\text{Gd,Nd})\text{Mg}$        | 66.4              | 32.5              | 50.3              | 49.4              |
|   | 66.3              | 31.9              | 50.2              | 48.7              |

intermetallic phase was found in the diffusion triple. According to the local equilibrium compositions in Table 2, combining with the BSE images in Fig. 3, a schematic diagram of the Mg–Nd–Gd diffusion triple at 723 K is illustrated in Fig. 4, where the lines indicate the interfaces between two single phases and the 4 connecting points indicate the 4 three-phase equilibria.

**Fig. 4** Schematic diagram of diffusion triple of Mg–Gd–Nd system at 723 K for 384 h

$\alpha(\text{Mg})$ ,  $\text{Mg}_7\text{Gd}$  and  $\text{Mg}_{41}\text{Nd}_5$  build a tri-phase equilibrium which is close to the pure magnesium (point 1 in Fig. 4).  $\text{Mg}_7\text{Gd}$ ,  $\text{Mg}_5\text{Gd}$  and  $\text{Mg}_{41}\text{Nd}_5$  establish a tri-phase equilibrium (point 2 in Fig. 4). Almost all the binary phases are linear compounds. It was found that the third elements can dissolve in those binary compounds to a determined degree. As a result, the  $\text{Mg}_3\text{Nd}$  and  $\text{Mg}_3\text{Gd}$  form a continuous solid solution named as  $(\text{Gd,Nd})_3\text{Mg}$ . It is not surprising that  $\text{Mg}_3\text{Nd}$  and  $\text{Mg}_3\text{Gd}$  can form a continuous solid solution, which can be represented as  $(\text{Gd,Nd})_3\text{Mg}$  phase. Both  $\text{Mg}_3\text{Nd}$  and  $\text{Mg}_3\text{Gd}$  have same crystal structure (shown in Table 1) and the atomic radii of Nd and Gd are very close. So, Nd and Gd can replace each other in  $(\text{Gd,Nd})_3\text{Mg}$  phase. The solid solubilities of Nd and Gd in  $(\text{Gd,Nd})_3\text{Mg}$  phase are definite in the three-phase reaction point 3 (shown in Fig. 4). The solubilities of Gd and Nd in  $(\text{Gd,Nd})_3\text{Mg}$  phase are ~6.2% Gd and ~17.9% Nd near this point, respectively. The diffusion layer of the  $\text{Mg}_2\text{Gd}$  phase is very thin; the thickness of the layer is just about 3  $\mu\text{m}$ . So enough time of the annealing is essential. The annealing time of this diffusion triple is suitable, the high-diffusion rate phase is not too thick and the thin phase also can be clearly detected.

The BSE images of this diffusion triple and composition analysis (EPMA) show that there is no clear phase boundary and composition-jumping between

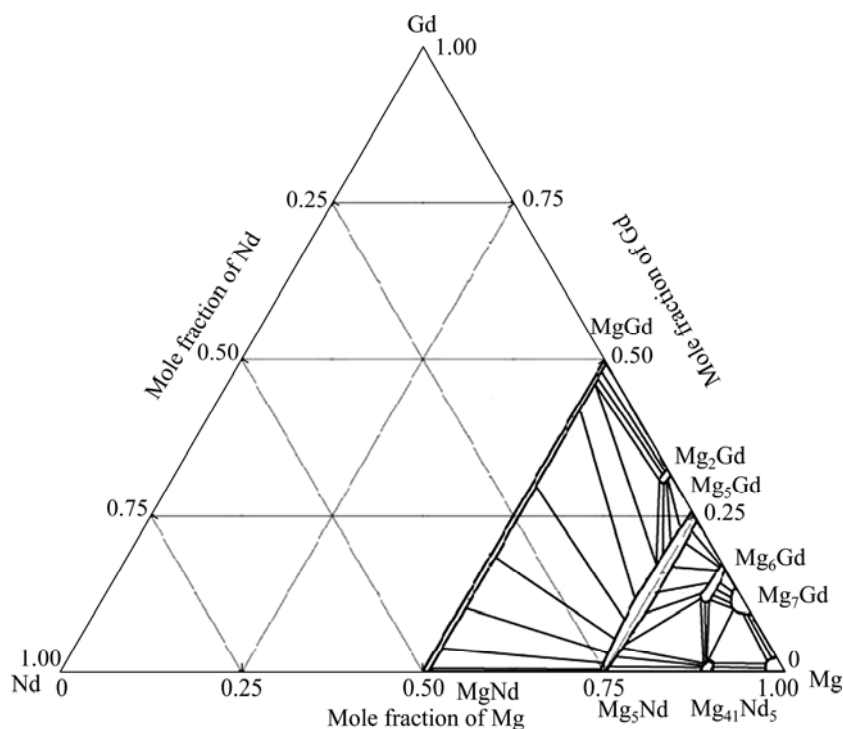


Fig. 5 Isothermal section of Mg–Nd–Gd ternary system at 723 K

MgNd and MgGd phase interface. Because the two intermediate phases have the same crystal structure (shown in Table 1) and the atomic sizes of Nd and Gd are similar, it can be concluded that the MgNd and MgGd form a continuous solid solution, which can be represented as (Gd,Nd)Mg. In the three-phase reaction point of (shown in Fig. 4), the equilibrium solubilities of Nd and Gd in (Gd,Nd)Mg are ~7.0% and ~43.0%.

All the tri-phase equilibria are concerned, and four tri-phase equilibria have been established,  $\alpha(\text{Mg}) + \text{Mg}_7\text{Gd} + \text{Mg}_{41}\text{Nd}_5$ ,  $\text{Mg}_7\text{Gd} + \text{Mg}_5\text{Gd} + \text{Mg}_{41}\text{Nd}_5$ ,  $\text{Mg}_5\text{Gd} + \text{Mg}_{41}\text{Nd}_5 + (\text{Gd,Nd})_3\text{Mg}$  and  $(\text{Gd,Nd})_3\text{Mg} + (\text{Gd,Nd})\text{Mg} + \text{Mg}_2\text{Gd}$  (shown in Fig. 3). An isothermal section of Mg–Nd–Gd ternary system at 723 K is shown in Fig. 5.

#### 4 Conclusions

1)  $\text{Mg}_7\text{Gd}$ ,  $\text{Mg}_5\text{Gd}$ ,  $\text{Mg}_2\text{Gd}$ ,  $\text{Mg}_{41}\text{Nd}_5$ ,  $(\text{Gd,Nd})_3\text{Mg}$  and  $(\text{Gd,Nd})\text{Mg}$  are formed in Mg–Nd–Gd ternary system. In these intermetallic phases, the  $\text{Mg}_7\text{Gd}$  phase has been reported to be metastable phase in the previous literatures.

2) The solubility values of Mg, Gd and Nd in all the phases were detected.

3) Four tri-phase equilibria were confirmed,  $\alpha(\text{Mg}) + \text{Mg}_7\text{Gd} + \text{Mg}_{41}\text{Nd}_5$ ,  $\text{Mg}_7\text{Gd} + \text{Mg}_5\text{Gd} + \text{Mg}_{41}\text{Nd}_5$ ,  $\text{Mg}_5\text{Gd} + \text{Mg}_{41}\text{Nd}_5 + (\text{Gd,Nd})_3\text{Mg}$  and  $(\text{Gd,Nd})_3\text{Mg} + (\text{Gd,Nd})\text{Mg} + \text{Mg}_2\text{Gd}$ .

#### References

- [1] WU Yu-juan, DING Wen-jiang, PENG Li-ming. Research progress of advanced magnesium rare-earth alloys [J]. Materials China, 2011, 30(2): 1–8.
- [2] DRITS M E, ZUSMAN L L, ROKHLIN L L. Influence of alloying elements on the velocity of ultrasound in magnesium [J]. Ultrasonics, 1971, 9(2): 123.
- [3] HOU Xiu-li, PENG Qiu-ming, CAO Zhan-yi, XU Shi-wei, KAMADO S, WANG Li-dong, WU Yao-ming, WANG Li-min. Structure and mechanical properties of extruded Mg–Gd based alloy sheet [J]. Materials Science and Engineering A, 2009, 520(1): 162–167.
- [4] SCHUMANN S, FRIEDRICH H. Current and future use of magnesium in the automobile industry [J]. Materials Science Forum, 2003, 419: 51–56.
- [5] WANG Feng, WANG Yue, MAO Ping-li, YU Bau-yi, GUO Quan-ying. Effects of combined addition of Y and Ca on microstructure and mechanical properties of die casting AZ91 alloy [J]. Transactions of Nonferrous Metals Society of China, 2010, 20: s311–s317.
- [6] LI De-jiang, ZENG Xiao-qin, XIE Yan-cai, WU Yu-juan, DING Wen-jiang, CHEN Bin. Mechanical properties of Mg–6Gd–1Y–0.5Zr alloy processed by low temperature thermo-mechanical treatment [J]. Transactions of Nonferrous Metals Society of China, 2012, 22: 2351–2356.
- [7] NAYEB-HASHEMI A A, CLARK A A. Phase diagrams of binary magnesium alloys metals park [M]. Ohio: ASM International, 1988.
- [8] DELFINO S, SACCONI A, FERRO R. Phase relationships in the neodymium–magnesium alloy system [J]. Metall Trans, 1990, 21(8): 2109–2114.
- [9] GORSSE S, HUTCHINSON C R, CHEVALIER B, NIE J F. A thermodynamic assessment of the Mg–Nd binary system using random solution and associate models for the liquid phase [J].

- Journal of Alloys and Compounds, 2005, 392: 253–262.
- [10] MENG Fan-gui, LIU Hua-shan, LIU Li-bin, JIN Zhan-peng. Thermodynamic optimization of Mg–Nd system [J]. Transactions of Nonferrous Metals Society of China, 2007, 17: 77–81.
- [11] GUO Cui-ping, DU Zhen-ming. Thermodynamic assessment of the Mg–Nd system [J]. Zeitschrift Fur Metallkunde, 2006, 97(2): 130–135.
- [12] ROKHLIN L L. Magnesium alloys containing rare earth metals: Structure and properties [M]. CRC Press, 2003: 43–45.
- [13] NISHIJIMA M, HIRAGE K, YAMASAKI M, KAWAMURA Y. Characterization of  $\beta'$  phase precipitates in an Mg–5at%Gd alloy aged in a peak hardness condition, studied by high-angle annular detector dark-field scanning transmission electron microscopy [J]. Materials Transactions, 2006, 47(8): 2109–2112.
- [14] ZHANG Lei, DONG Xuan-pu, LI Ji-qiang, WANG Wen-jun, WANG Ai-hua, FAN Zi-tian. Microstructure and mechanical properties of as-cast and heat treated Mg–15Gd–3Y alloy [J]. Journal of Rare Earths, 2011, 29(1): 77–82.
- [15] LIU H, GAO Y, LIU J Z, ZHU Y M, WANG Y, NIE J F. A simulation study of the shape of  $\beta'$  precipitates in Mg–Y and Mg–Gd alloys [J]. Acta Materialia, 2013, 61: 453–466.
- [16] GILL L R, LORIMER G W, LYON P. The effect of zinc and gadolinium on the precipitation sequence and quench sensitivity of four Mg–Nd–Gd alloys [J]. Advanced Engineering Materials, 2007, 9(9): 784–792.
- [17] CHEN Ping, LI Dong-lin, YI Jian-xiong, WEN Li, TANG Bi-yu, PENG Li-ming, DING Wen-jiang. Structural, elastic and electronic properties of  $\beta'$  phase precipitate in Mg–Gd alloy system investigated via first-principles calculation [J]. Solid State Sciences, 2009, 11(12): 2156–2161.

## Mg–Nd–Gd 三元系 723 K 的等温截面

肖 龙<sup>1</sup>, 钟 燕<sup>1</sup>, 陈翠萍<sup>1</sup>, 吴刘明明<sup>1</sup>, 罗天旷<sup>1</sup>, 刘立斌<sup>1,2</sup>, 林 葵<sup>3</sup>

1. 中南大学 材料科学与工程学院, 长沙 410083;

2. 中南大学 有色金属材料科学与工程教育部重点实验室, 长沙 410083;

3. 广西分析测试研究中心, 南宁 530022

**摘 要:** 采用三元扩散偶技术, 利用电子探针成分分析, 建立 Mg–Nd–Gd 三元系 723 K 的等温截面。Mg<sub>3</sub>Gd 和 Mg<sub>3</sub>Nd 在三元系中形成连续固溶体(Gd,Nd)<sub>3</sub>Mg, MgGd 和 MgNd 也形成连续固溶体(Gd,Nd)Mg。在三元系中出现的金属间化合物有 Mg<sub>7</sub>Gd、Mg<sub>5</sub>Gd、Mg<sub>2</sub>Gd、Mg<sub>41</sub>Nd<sub>5</sub>、(Gd,Nd)<sub>3</sub>Mg 和(Gd,Nd)Mg, 其中 Mg<sub>7</sub>Gd 在以往报道中认为是亚稳相。测量了 Mg、Gd 和 Nd 在每相中的溶解度, 发现在 Mg–Nd–Gd 三元系中存在 4 个三相平衡, 它们分别是  $\alpha(\text{Mg})+\text{Mg}_7\text{Gd}+\text{Mg}_{41}\text{Nd}_5$ ,  $\text{Mg}_7\text{Gd}+\text{Mg}_5\text{Gd}+\text{Mg}_{41}\text{Nd}_5$ ,  $\text{Mg}_5\text{Gd}+\text{Mg}_{41}\text{Nd}_5+(\text{Gd,Nd})_3\text{Mg}$  和  $(\text{Gd,Nd})_3\text{Mg}+(\text{Gd,Nd})\text{Mg}+\text{Mg}_2\text{Gd}$ 。

**关键词:** 镁合金; Mg–Nd–Gd 三元系; 三元扩散偶; 相图; 等温截面

(Edited by Hua YANG)